Ionization of Aromatic Sulfides in Nonpolar Media: Free vs Reaction-Controlled Electron Transfer

Nikolaos Karakostas,[†] Sergej Naumov,[‡] and Ortwin Brede*,[†]

Interdisciplinary Group for Time-Resolved Spectroscopy, University of Leipzig, Permoserstrasse 15, 04303 Leipzig, Germany, and Institute of Surface Modification, 04303 Leipzig, Germany

Received: October 9, 2006; In Final Form: November 2, 2006

The primary products of the bimolecular free electron transfer (FET) from aromatic sulfides ($PhSCH_2Ph$, $PhSCHPh_2$, $PhSCPh_3$) to *n*-butyl chloride radical cations are two radical cation conformers: a dissociative and a metastable one. In analogy with formerly studied donor systems, this result seems to reflect femtosecond oscillations in the ground state of the sulfides such as torsion motions around the Ar−S bond. This motion is accompanied by a marked electron fluctuation within the HOMO (or the n) orbitals. The FET products observed in the nanosecond time scale such as the metastable sulfide radical cations ($Ar-S-CR_3^{\bullet+}$), the dissociation products R_3C^+ and $R_3C^{\bullet}$, and their (experimentally) nondetectable counterparts $Ar-S^{\bullet}$ as well as $Ar-S^+$ can be understood with the simplified assumption of two extreme conformations, namely a planar and a twisted donor molecule. Using mediator radical cations (benzene, butylbenzene, biphenyl), the stepwise reduction of the free energy of the electron transfer from $-\Delta H = 2.5$ to ≤ 0.5 eV changes the dissociation pattern of the sulfide radical cations toward a uniform product such as the metastable sulfide radical cation. From that, we tentatively interpret the mechanism of the studied electron transfer as diffusion-controlled (collision-determined FET) at higher $-\Delta H$ values and as reaction-controlled at $-\Delta H$ below 0.5 eV.

1. Introduction

The parent radical cations produced in the radiolysis of alkyl chlorides (here *n*-BuCl, reaction 1a) and alkanes are powerful oxidants that are able to generate a vast number of secondary radical cations.[1] They ionize molecules having lower ionization potentials than theirs (IP ≈ 9.5−10.5 eV), and hence they appear to be universal tools for the generation of solute radical cations.[2−4] Usually, this kind of one-electron oxidation is a diffusion-controlled reaction that is called free electron transfer (FET) (eq 1b).[5]

$$n\text{-BuCl} \rightsquigarrow [n\text{-BuCl}^{\bullet+} + e_{solv}^{-}] \rightarrow n\text{-BuCl}^{\bullet+} + Bu^{\bullet} + Cl^{-} \quad (1a)$$

$$n\text{-BuCl}^{\bullet+} + D \rightarrow (FET) \rightarrow n\text{-BuCl} + D^{\bullet+} \quad (D = \text{electron donor}) \quad (1b)$$

The nonpolar nature of the environment diminishes the stabilization of the ions by solvation. FET takes place without the formation of an encounter complex in the typical sense. It is a very exergonic process. Every collision of the reactants leads to an electron jump regardless of their relative geometry. Therefore, the overall rate is determined by the diffusion of the transients and the detection resolution is limited to the nanosecond time scale. However, the electron jump itself is faster than molecular motions. Consequently, the reactants do not receive a favorable conformation during the process and the (immediate) products preserve the geometry of their precursors. The substrates that are affected the most from these reaction conditions are aromatic compounds with highly mobile substituents. When its rotation barrier is small enough, the molecules can be found in all spatial arrangements about single bonds. These torsion motions of the substituents are accompanied by considerable fluctuation of the electrons in the highest molecular orbitals. Simplifying this complex behavior, two extreme conformers (planar and vertical) are defined, which serve as models for molecules undergoing FET, as shown in Scheme 1.

The borderline structures of Scheme 1 provided the means for understanding the FET reaction involving, e.g., phenols. Radiolysis of phenol (ArOH) in alkane and alkyl chloride (RX) solutions produces comparable amounts of phenol radical cations and phenoxyl radicals which are formed simultaneously:[5−7]

$$ArOH_{planar\,(\parallel)} \longrightarrow ArOH^{\bullet+}* \longrightarrow ArOH^{\bullet+} \quad (2a)$$

$$RX^{\bullet+} + \text{Ar-}\circlearrowleft\text{-OH} + RX$$

$$ArOH_{vertical(\perp)} \longrightarrow [Ar\text{-}O^{\bullet+}\text{-}H]* \longrightarrow ArO^{\bullet} + H^{+} \quad (2b)$$

Each reaction channel in eqs 2a and 2b arises from dissimilar orientations of the OH group relative to the phenyl plane. The radical cations of thiols,[7] aromatic amines[8,9] and aromatic silanes[10,11] also exhibit stabilities which are different in the case of "vertical" and "planar" conformers. The FET properties were recently featured in this Journal.[12]

Aromatic sulfides constitute a group of molecules that fulfills the structural conditions described above. They exhibit a low barrier to rotation about the $C_{sp^2}-S$ bond[13−15] and their ionization potential (∼7.9 eV[16,17]) is much below that of *n*-BuCl

* Corresponding author. E-mail address: brede@mpgag.uni-leipzig.de.
[†] University of Leipzig.
[‡] Institute of Surface Modification.

10.1021/jp066619q CCC: $37.00
Published on Web 12/14/2006

SCHEME 1

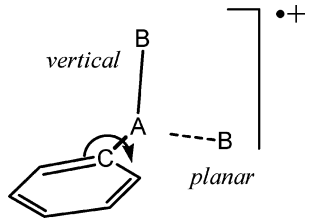

SCHEME 2

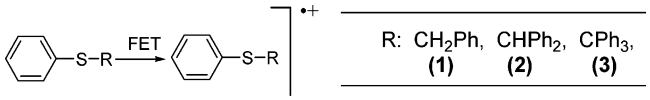

(10.8 eV[18]). Up to now, the chemical behavior of aromatic sulfides' radical cations has not received the same attention as that of the aliphatic sulfides. Even their ability to form two-center three-electron "dimers" is a subject of debate.[19−22] Dissociation of the S−C bond and deprotonation in β position to the S atom are the best known reactions occurring after the electron transfer in polar systems.[23−26] The purpose of this paper is to describe the very peculiar free electron-transfer properties (Scheme 2) of them.

2. Experimental Section

Materials. *n*-Butyl chloride was purified by treatment with molecular sieves (A4, X13) and distillation as previously described.[6,27] Triphenylmethyl phenyl sulfide (**3**) was prepared by reaction of thiophenol and triphenyl chloride (Aldrich) in benzene under reflux.[25] Diphenylmethyl phenyl sulfide (**2**) and benzyl phenyl sulfide (**1**) were produced by coupling of $PhCH_2$-Cl and Ph_2CHCl with ethanolic PhS^-. All compounds were recrystallized twice from EtOH.

Pulse Radiolysis. The samples were purged with N_2 or O_2 and irradiated with electron pulses (1 MeV, 15 ns duration) delivered from a pulse transformer electron accelerator ELIT (Institute of Nuclear Physics, Novosibirsk, Russia). Dosimetry was performed using the absorption of the solvated electron in water and corresponds to a dose around 100 Gy. Optical detection of transients involved a xenon lamp (XBO 450, Osram), a SpectraPro- 500 monochromator (Acton Research Corp.), a R955 photomultiplier (Hamamatsu Photonics) and a 1 GHz digitizing oscilloscope (TDS 640, Tektronix).[6] The solutions were continuously passed through the sample cell. The cell length was 1 cm.

Quantum Chemical Calculations. Quantum chemical calculations were performed with density functional theory (DFT) Hybrid B3LYP methods[28−30] and standard 6-31G(d) basis set as implemented in the Gaussian 03 program.[31]

3. Results

Pulse Radiolysis Experiments. *Diphenylmethyl Phenyl Sulfide (2).* Pulse radiolysis of pure *n*-BuCl results in the formation of the well-known broad absorption band of n-$BuCl^{\bullet+}$ with maximum at 500 nm.[3] These parent radical cations have a lifetime of approximately 100 ns. The addition of a quencher in millimolar concentration shortens it down to ~40 ns ($k \sim 1.5 \times 10^{10}$ dm^3 mol^{-1} s^{-1}) (cf. eq 1b). In particular, when diphenylmethyl phenyl sulfide (**2**) was employed, a well structured spectrum of at least two transients was initially observed (see open circles in Figure 1a). They appear simultaneously as the *n*-$BuCl^{\bullet+}$ (seen as a spike in the insets of Figure 1a) decays.

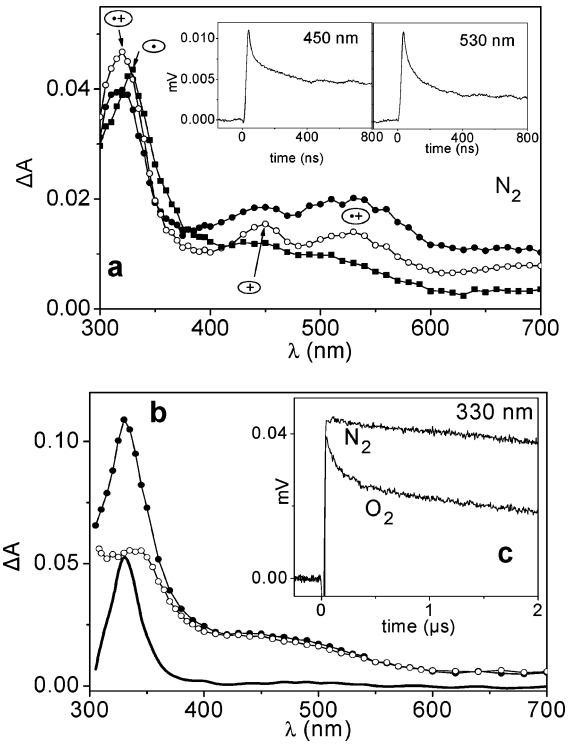

Figure 1. Absorption spectra recorded after pulse radiolysis of sulfide **2** in *n*-BuCl. (a) 5×10^{-4} mol dm^{-3} solution saturated with N_2: 80 ns (●), 200 ns (○), 1 μs (■) after the pulse. Insets are time profiles at 450 and 530 nm. (b) 5×10^{-3} mol dm^{-3} solution 1.5 μs after the pulse under N_2 (●) and under O_2 (○) and their difference spectrum (continuous line). (c) Corresponding time profiles at 330 nm under N_2 and O_2 atmosphere.

The peaks at 320 and 530 nm (τ = 140 ns) belong to the radical cation of **2**. The assignment was made on the basis of the similarity with the absorption of the other sulfide radical cations,[20,23,32] and their sensitivity toward nucleophiles. Oxygen has a marginal influence on the lifetime of the transient. The second species, with a maximum at 450 nm and a lifetime of 130 ns belongs to the diphenylmethyl cation.[33,34] The parent molecule has a quenching effect on this cation (in addition to that of nucloephiles), as presented in

$$Ph_2C^+ + \mathbf{2} \rightarrow \text{products} \qquad (3)$$

When the concentration of **2** exceeds 1×10^{-3} mol dm^{-3}, the band at 450 nm disappears. This is attributed to the interaction of Ph_2CH^+ with the aromatic rings of the sulfide and to its electrophilic properties.

As can be seen in Figure 1a, 1 μs after the pulse the main absorption band shifts to 330 nm. This corresponds to the formation of the diphenylmethyl radical. Oxygen quenches the transient observed at 330 nm (Figure 1c) with a rate constant $k = (1.2 \pm 0.2) \times 10^9$ dm^3 mol^{-1} s^{-1}, which is typical for the peroxidation of carbon-centered radicals. The spectrum of the radical[33,35,36] is given by the difference between those taken in N_2 and in O_2 purged solutions, cf. continuous line in Figure 1b.

Triphenylmethyl Phenyl Sulfide (3). When a 1×10^{-3} mol dm^{-3} solution of trityl phenyl sulfide in *n*-BuCl saturated with N_2 is subjected to pulse radiolysis, then FET to parent *n*-$BuCl^{\bullet+}$ results primarily in the generation of the corresponding radical cations. However, their presence cannot be detected because of the short lifetime. An upper limit of 25 ns can be estimated on the basis of the lifetime of *n*-$BuCl^{\bullet+}$. In Figure 2a, the intense

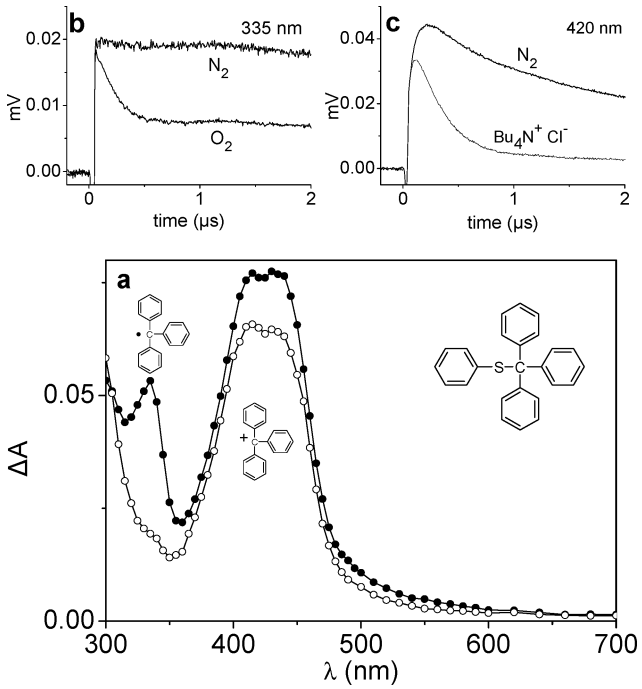

Figure 2. Absorption spectra recorded 1 μs after pulse radiolysis of a 1×10^{-3} mol dm^{-3} solution of triphenylmethyl phenyl sulfide **3** in *n*-BuCl purged with N_2 (●) and with O_2 (○) (a). Time profiles taken at 335 nm under N_2 and O_2 atmosphere (b) and at 420 nm in the absence and in the presence of 2×10^{-4} mol dm^{-3} Bu_4NCl (c).

twin band with maximum at 420 and 435 nm is assigned to the trityl cation.[37] It is not sensitive to oxygen (Figure 2a, open circles) but reacts promptly with nucleophiles. In eq 4 and Figure 2c the nucleophile is Cl^-. Furthermore, the sharp peak at 335

$$Ph_3C^+ + Cl^- \rightarrow Ph_3CCl \qquad k = (1.6 \pm 0.3) \times 10^{10}\ dm^3\ mol^{-1}\ s^{-1} \quad (4)$$

nm is attributed to the formation of the trityl radical $Ph_3C^{\bullet}$.[37,38] Its reaction with oxygen ($k = (9 \pm 1) \times 10^8$ dm^3 mol^{-1} s^{-1}) can be derived from the time profiles given in Figure 2b. Both transients observed (Ph_3C^+ and $Ph_3C^{\bullet}$) originate from the same part of the fragmented radical cation $\mathbf{3}^{\bullet+}$ and appear simultaneously. That is an indication for the existence of two reaction channels. Because their extinction coefficients are known[33] (ϵ_{430} = 38 000 mol^{-1} dm^3 cm^{-1} for Ph_3C^+, ϵ_{334} = 36 000 mol^{-1} dm^3 cm^{-1} for $Ph_3C^{\bullet}$) the product ratio can be estimated from their time profiles: The difference in the absorption at 335 nm, caused by O_2, is proportional to the concentration of the trityl radical, whereas the difference in the absorption at 420 nm, due to $Bu_4N^+Cl^-$, is proportional to the concentration of the trityl cation. In this way, a 3:1 ratio between cation and radical production was derived from Figure 2b,c.

Stepwise Electron Transfer from Triphenylmethyl Phenyl Sulfide. The radical cations of sulfides can also be generated by stepwise electron transfer using an intermediate molecule for the first stage, as formulated in the reaction sequence (5) and (6). The intermediate should exhibit an ionization potential between that of *n*-BuCl and the target molecule (the sulfide) so that the process is feasible and efficient.

$$n\text{-BuCl}^{\bullet+} + PhH \rightarrow PhH^{\bullet+} + n\text{-BuCl} \quad (5)$$

$$PhH^{\bullet+} + PhSCPh_3 \rightarrow PhH + PhSCPh_3^{\bullet+} \quad (6)$$

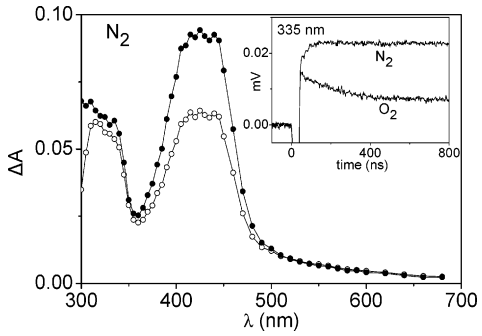

Figure 3. Absorption spectra recorded on pulse radiolysis of a 1×10^{-3} mol dm^{-3} solution of triphenylmethyl phenyl sulfide and 0.5 mol dm^{-3} benzene in *n*-BuCl saturated with N_2: 90 ns (●) and 150 ns (○) after the pulse. Insets are time profiles at 335 nm under N_2 and O_2 atmosphere.

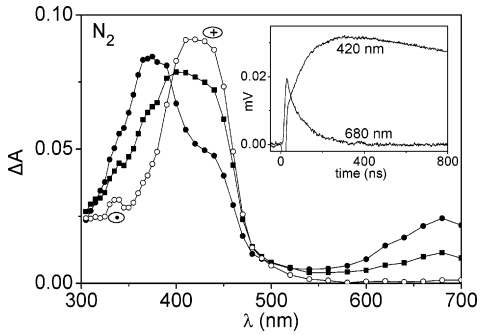

Figure 4. Transient spectra recorded after pulse radiolysis of a 1×10^{-3} mol dm^{-3} solution of triphenylmethyl phenyl sulfide and 1×10^{-2} mol dm^{-3} biphenyl in *n*-BuCl saturated with N_2: 80 ns (●), 150 ns (■), and 350 ns (○) after the pulse. Insets are time profiles at 420 and 680 nm.

Benzene (IP = 9.24 eV)[39] was used as a midway charge transporter in the radiolysis experiment documented in Figure 3. The addition of 0.5 mol dm^{-3} of benzene in N_2 purged *n*-BuCl causes the rapid formation of $PhH^{\bullet+}$ (in equilibrium with its dimer),[40,41] according to reaction 5, which in turn ionizes **3,** reaction 6. The radical $Ph_3C^{\bullet}$ and the cation Ph_3C^+ are identified as described in the previous paragraph. They appear with almost the same ratio ($[Ph_3C^+]/[Ph_3C^{\bullet}] = 3/1$) as in the case of direct ionization from the solvent radical cation. The intermediate radical cation $PhH^{\bullet+}$ cannot be directly observed because it absorbs in the spectral range around 450 nm with a much smaller extinction coefficient than for the trityl species.

Biphenyl (IP = 8.34 eV)[42] was used as intermediate oxidizer in the pulse radiolysis spectra described in Figure 4. After FET (eq 7) the radical cation $PhPh^{\bullet+}$ (monomeric form initially) appears with λ_{max} at 365 and 680 nm, in agreement with previous reports.[1,43] The addition of compound **3** in millimolar concentration reduces its lifetime from 0.7 μs to 90 ns (reaction 8). The dissociation product of eq 9, the trityl cation, is growing in with the same time law (inset of Figure 4).

$$n\text{-BuCl}^{\bullet+} + PhPh \rightarrow PhPh^{\bullet+} + n\text{-BuCl} \quad (7)$$

$$PhPh^{\bullet+} + PhSCPh_3 \rightarrow PhPh + PhSCPh_3^{\bullet+} \quad (8)$$

$$PhSCPh_3^{\bullet+} \rightarrow PhS^{\bullet} + Ph_3C^+ \quad (9)$$

The minor peak at 335 nm observed 350 ns after the pulse is due to the $Ph_3C^{\bullet}$ radical and can be eliminated under oxygen atmosphere. It can be calculated (from the absorption spectra

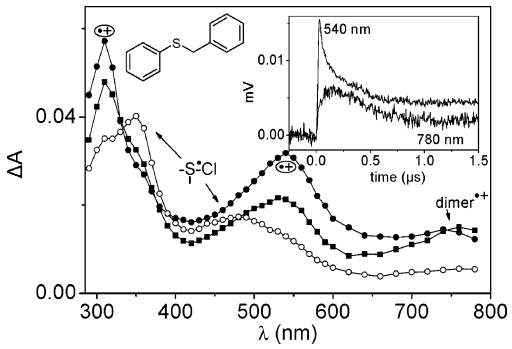

Figure 5. Absorption spectra recorded on pulse radiolysis of a 1×10^{-3} mol dm^{-3} solution of benzyl phenyl sulfide **1** in *n*-BuCl purged with N_2: 80 ns (●), 200 ns (■), and 1 μs (○) after the pulse. The inset contains representative time profiles.

and the time profiles of the species) that the relative amount of trityl cation to trityl radical produced is 15/1.

Benzyl Phenyl Sulfide (1). The pulse radiolysis of a 1×10^{-3} mol dm^{-3} solution of compound **1** in N_2 purged *n*-BuCl results in the spectra given in Figure 5. Initially, two absorption bands (with λ_{max} at 310 nm and at 540 nm) were formed (reaction 10), which we assign to the radical cation $\mathbf{1}^{\bullet+}$. Both peaks show

$$n\text{-BuCl}^{\bullet+} + \text{PhSCH}_2\text{Ph} \rightarrow \text{PhSCH}_2\text{Ph}^{\bullet+} + n\text{-BuCl} \quad (10)$$

identical kinetics in N_2 purged solution ($\tau = 130$ ns). Oxygen has no noticeable effect on the band at 540 nm whereas the spectral range around 310 nm is masked by butylperoxyl radicals.

The broad band with a maximum at 780 nm corresponds to the charge-transfer dimer of the radical cation. A similar behavior was reported recently by Baciocchi et al. for the photosensitized oxidation of benzyl phenyl sulfide in MeCN.[44] We found that at constant dose per electron pulse: (a) the decay rate of $\mathbf{1}^{\bullet+}$ is practically the same as that of its dimer (inset of Figure 5), (b) the concentration of **1** (5×10^{-4} to 1×10^{-2} mol dm^{-3}) has no influence on the decay rate of $\mathbf{1}^{\bullet+}$, and (c) the amount of dimer produced is proportional to the concentration of **1**. This indicates that the monomeric and the dimeric radical cations are in equilibrium as described by:

$$\text{PhSCH}_2\text{Ph}^{\bullet+} + \text{PhSCH}_2\text{Ph} \rightleftharpoons [\text{PhSCH}_2\text{Ph}]_2^{\bullet+} \quad (11)$$

The time evolution of the absorption spectra shows that the decay of the radical cation is accompanied by the formation of two bands ($\lambda_{max} = 350$ and 480 nm). Both peaks belong to the adduct of $\mathbf{1}^{\bullet+}$ and Cl^-, cf. reaction 12. The origin of the chloride

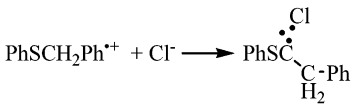

(12)

anion is the radiolysis of *n*-BuCl (eq 1a). The identification of the adduct was based on (a) the acceleration of the formation of the adduct upon Cl^- addition (in the form of tetrabutylammonium chloride) and (b) in the shift of λ_{max} (from 350 to 365 nm) when the bromine anion was employed.

Dissociation of $\mathbf{1}^{\bullet+}$ could not be established. Because the possible dissociation products ($PhCH_2^{\bullet}$, $\lambda_{max} = 316$ nm;[45] $PhCH_2^{\bullet+}$, $\lambda_{max} = 303$ nm[46]) absorb at the same spectral range as the parent radical cation, their direct observation would be significantly hindered.

4. Discussion

The experimental results associated with FET in sulfides indicate that there are two distinct channels for the dissociation of the C−S bond of the radical cations (which are originally derived from *n*-BuCl$^{\bullet+}$). This is depicted in the spectra of Figures 1−4 (can be best verified from Figure 2). The cleavage occurs with the formation of radical and cationic fragments. The generation of two types of radical cations, with the same configuration but different spin distribution, is a key concept given in Scheme 3. Both radical cations dissociate, resulting in transients that can be clearly identified from their optical absorption properties.

Preceding reports of free electron transfer in phenols[7] (reactions 1 and 2), amines[8] and silanes[11] have established the connection between molecular conformation and stability of the transient radical cation; see also ref 12. In this context it is helpful if the electron transfer is subdivided in individual reaction steps as shown in the following sequence:

$$RX^{\bullet+} + D \xrightarrow{\text{approach}} RX^{\bullet+}...D \xrightarrow{\text{e-jump}} RX...D^{\bullet+} \xrightarrow{\text{diffusion}} RX + D^{\bullet+} \quad (13)$$

The gross reaction itself is kinetically characterized by the diffusional approach as the slowest step. During this time the donor molecule (D) is in standing oscillation. In the case of aromatic moieties with characteristic rotating substituents, the oscillation means also that a standing mixture of conformers exists. It is conditioned by the electron fluctuation connected with the bending motion. The electron jump itself is extremely rapid and proceeds in times ≤ 1 fs. The electron jump thus occurs from a donor molecule in its momentary rotation state and results in the corresponding donor radical cation.

FET is such a rapid process that it can trigger chemical phenomena that originate from different rotational isomers. In the case of phenol radical cations $PhOH^{\bullet+}$ generated in FET, the vertically positioned OH group deprotonates much faster (within the first vibration motions, ~10 fs) than the planar form of the transient, which is a metastable radical cation (see eqs 2a and 2b and Scheme 1).

The electron transfer from aromatic sulfides to *n*-BuCl$^{\bullet+}$ fulfils the required conditions described above for FET. As a result of the rapid (vertical) ionization process, the radical cation is generated in the same configuration as the ground state molecule. Because the rotation barrier is very small, the phenyl group attached to the S atom does not have a favorable orientation with respect to the S−C_{sp^3} bond. After the electron loss the S−C_{sp^3} bond is weak ($E_{dis} = 35$ kJ/mol for $\mathbf{3}^{\bullet+}$) and dissociation takes place with the separation between spin and charge. In such a case two main questions emerge: (i) what factors determine the direction of the fragmentation into radical and cationic residue, and (ii) can the ratio of products be altered?

Interpretation of Product Distribution after FET. With asymmetric radical cations the cleavage may give alternative pairs of cations and radicals. Under conditions of thermodynamic equilibrium, the cation is preferably derived from the radical fragment with the lower ionization potential.[47] For compound **2** the diphenylmethyl cation is the most likely one to be formed.

To exclude the possibility of parallel reactions, in which a reactant (a single radical cation) undergoes independent, concurrent reactions, we could calculate[48] for the reactions paths (14) and (15) of Scheme 3 the ratio $k_{15}/k_{14} = [Ph_2CH^{\bullet}]/[Ph_2CH^+]$.

SCHEME 3

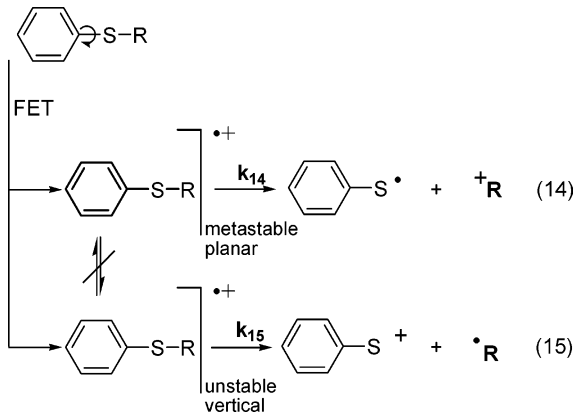

TABLE 1: Vertical Ionization Potentials and Reaction Parameters of Intermediate Electron Donors[a]

	$IP_{vertical}$ (eV)	$k_{sulfide}$ ($dm^3\ mol^{-1}\ s^{-1}$)	product ratio: $Ph_3C^•/Ph_3C^+$
n-BuCl	10.84 (ref 18)	1.2×10^{10}	25/75
PhH	9.25 (ref 39)	1.0×10^{10}	25/75
PhBu	8.69 (ref 52)	1.1×10^{10}	25/75
PhPh	8.34 (ref 42)	9.3×10^{9}	6/94

[a] $k_{sulfide}$ is the rate constant for the electron transfer from compound **3** to the radical cations.

From the Arrhenius equation (assuming a common frequency factor A) we can also derive $k_{15}/k_{14} = e^{-(E_{15}-E_{14})/RT}$, where k_{14} and k_{15} are the rate constants, E_{14} and E_{15} are the dissociation energies of the reactions, R is the gas constant, and T is the absolute temperature. By substituting the calculated dissociation energies from Table 2, we get $[Ph_2CH^•]/[Ph_2CH^+] = 10^{-36} \approx 0$.

The great difference in the ionization potentials ($\Delta IP = IP_{PhS^•} - IP_{Ph_2CH^•} = 8.6$ eV[49] $- 7.3$ eV[50] $= 1.3$ eV) should totally block the formation of $Ph_2CH^•$. In contrast to this calculation, the diphenylmethyl radical is effortlessly detected in the spectrum of Figure 1. Hence, we conclude that the two dissociation channels originate from different radical cations as presented in Scheme 3. The cation Ph_2CH^+ is detected qualitatively. Its short lifetime and high reactivity does not facilitate the calculation of the relative yields for the two transients. Unlike the carbon-centered transients ($Ph_2CH^•$, $\epsilon_{330} = 43\ 600$[33] and Ph_2CH^+, $\epsilon_{449} = 38\ 000$[34]) that were positively identified, the sulfur-containing fragments either have a small extinction coefficient ($PhS^•$ $\epsilon_{460} = 1800$[23]) or are reactive with nucleophiles (PhS^+)[51] and cannot be observed.

In an analogous manner the one electron oxidation of the sulfide **3** results in the fragmentation products Ph_3C^+ and $Ph_3C^•$. The ionization potential of the trityl radical ($IP_{Ph_3C^•} = 7.26$ eV)[37] is very similar to that of the diphenylmethyl radical, and the arguments concerning **2** can be applied to **3** as well. The ratio between reactions 14 and 15 is about 75% and 25%, respectively. The dissociation route of reaction 15 does not occur in polar solvents (water,[23] MeCN[24,44]) and appears to take place instantly (within the time range of electron transfer). It is introduced under typical FET conditions. The overall process should be analyzed in terms of the elementary steps as follows (see also reaction 13):

(1) The *diffusional approach* of the reactants. It is the slowest step of the procedure and determines the observed rate constant ($k = (1-2) \times 10^{10}$ $dm^3\ mol^{-1}\ s^{-1}$ for aromatic sulfides).

(2) The *electron jump* from the sulfide to *n*-$BuCl^{•+}$. This takes place very fast. There is no pre-association (encounter complex) between the reactants. Any collision is effective regardless of the encounter geometry or the conformation of the sulfide. The electron transfer is not followed by reorganization of the environment of the reactants; as in nonpolar systems, the solvation effects are very limited.

(3) *Distribution of the excessive energy* to the surrounding molecules and separation of the species.

A fraction of the sulfide radical cations are generated in *unstable* configurations that dissociate within the first vibrational motions (in some femtoseconds). This process is faster than the stabilizing rotational motion about the Ph−S bond (of the picosecond time scale in Table 2). When steps 2 and 3 are taking place simultaneously with the fragmentation of the radical cation, the gross reaction is exothermic and that can justify the unusual fragmentation pattern of

$$n\text{-BuCl}^{•+} + \text{PhSCPh}_3 \xrightarrow{\text{FET}} n\text{-BuCl} + \text{Ph}_3\text{C}^• + \text{PhS}^+ \qquad \Delta E = 69\ \text{kJ/mol} \quad (16)$$

On the other hand, the relaxed *metastable* radical cations have a lifetime of a few hundreds of nanoseconds and their dissociation falls within the typical reaction scheme of spin-charge separation of eq 14.

Effect of Intermediate Radical Cations on FET. The observation of unusual fragmentation patterns of the radical cations has been considered to be a special characteristic of FET. A deeper experimental analysis requires the investigation of the factors associated with this phenomenon. The most profound one is the nature of the parent radical cation. In its simplest form it is just the radical cation of the solvent. Alternatively, a molecule with an ionization potential (IP) lower than that for the solvent can be used as an intermediate in a first electron-transfer reaction, followed by a second electron transfer from the aromatic sulfides as described in reactions 5 and 6. The molecules employed appear in the left column of Scheme 4. Their vertical IP_{gas} values are known from the literature (see Table 1) and originate from photoelectron spectroscopy. The IP used for aromatic sulfides (7.9 eV)[16] corresponds to $PhSCH_2$-Ph, but no significant difference is expected for the other sulfides.

All the molecules used as mediator charge carriers are aromatics. Their radical cations have lifetimes sufficient ($\tau > 100$ ns) for the interaction with the sulfides under the experimental conditions. Phenyl trityl sulfide is the most appropriate molecule for the study of the complex kinetics of electron transfer because both of its carbon-centered fragments (cation and radical) can be conveniently monitored by UV spectroscopy. Benzene (Figure 3) and butylbenzene (Figure 6) give the same proportion between trityl radical and trityl cation as *n*-BuCl (25% and 75%, respectively). Unlike eq 16, the reaction is no longer exothermic (with the use of a mediator radical cation), so energetic considerations must not be regarded as the only reasons behind the general reaction scheme. A significant change in the reaction pattern occurs with biphenyl: The contribution of trityl radical is reduced to approximately 6%; cf. Figure 4.

The difference in IP between butylbenzene and the sulfide **3** is $\Delta IP = 0.8$ eV. Free energy differences in the range 0.5−2.0 eV were typical in the studies of FET mentioned previously. We can conclude that benzene and butylbenzene radical cations act in a way similar to that of *n*-$BuCl^{•+}$; therefore they are all placed in the area of the FET inducing oxidizers in Scheme 4. Biphenyl radical cations generate far less trityl radicals, indicating a modification of the reaction pathways. The channel of eq 15 is missing now. As a result, electron transfer from the sulfide

TABLE 2: DFT B3LYP/6-31G(d) Calculated Quantum Chemical Parameters[a]

		planar[b] radical cation		vertical[b] radical cation		E_{diss} (kJ/mol)		$10^{15}t$ (s)		E_a (kJ/mol)	
	S−C ground state (Å)	spin (*S*)	S−R (Å)	spin (*S*)	S−R (Å)	$ArS^+ + R^\bullet$	$ArS^\bullet + R^+$	rotation	valence	ground state	radical cation
$PhSCH_2Ph$	1.866	0.455	1.863	0.557	1.853	288	153	2080	51	1.2	39
$PhSCHPh_2$	1.881	0.458	1.888	0.527	1.880	261	53	2050	77	2.3	34
$PhSCPh_3$	1.941	0.542	2.045	0.535	2.072	215	35	850	64	2.8	∼44

[a] Bond lengths, spin density, dissociation energies, period of bending (torsion) and valence (stretching) oscillations of the S−C Bond and activation energy for the rotation around the Ph−S bond. [b] Named according to Scheme 1.

SCHEME 4

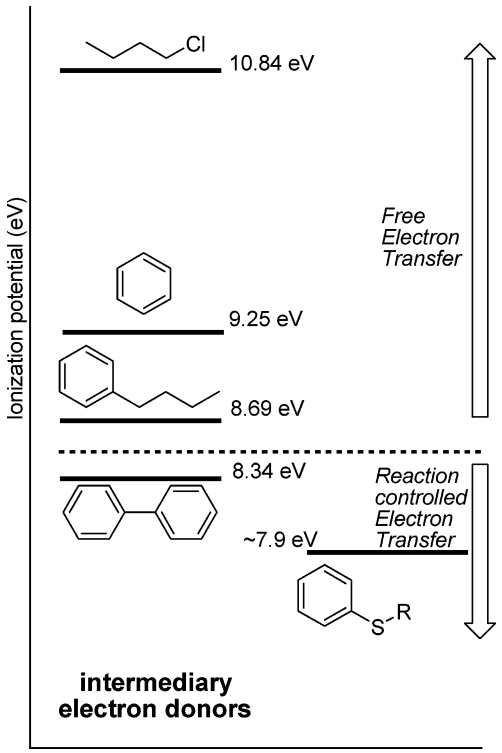

yields the trityl cation, which represents the product of the "reaction-controlled" electron transfer.[23,44] The IP difference between biphenyl and the sulfide is slightly smaller than 0.5 eV. That appears to be below the border for deactivation of the reaction 15.

The kinetic consequences of the IP difference between the electron donor and the acceptor have been established in previous studies of FET: The relation between the ionization potential difference and the rate constants k_{ET} of charge transfer from alkane and alkyl chloride radical cations to various solutes have been explained on the basis of the electron jump probability.[3,4] Then the Franck−Condon principle was used to describe the transition from the initial to the final cation−scavenger system. The calculated k_{ET} versus ΔIP curves correlate very well with the experimental ones. For scavengers with ΔIP up to 0.8 eV the results unambiguously pointed to an increase of k_{ET} with ΔIP. At ΔIP ≥ 0.8 eV the rate constants reach the diffusion-controlled limit and a plateau-like behavior was found. This behavior is illustrated for the case of the electron transfer from various solutes to $CCl_4^{\bullet+}$ (Figure 7), as already reported in refs 3 and 4.

Interestingly the plateau was in a similar IP range as the switch in the reaction mechanism that is observed for electron transfer from sulfides (as can be seen in Scheme 4). Moreover, FET from phenol described by reaction 2a,b can be adopted

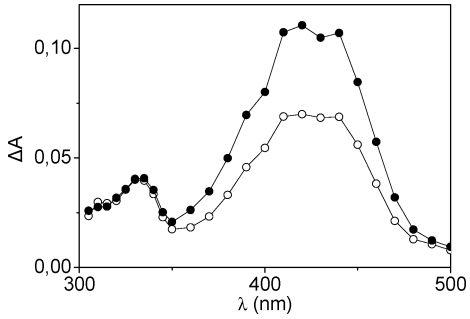

Figure 6. Absorption spectra taken 200 ns (●) and 1.5 μs (○) after pulse radiolysis of a 1×10^{-3} mol dm^{-3} solution of triphenylmethyl phenyl sulfide **3** with 1×10^{-2} mol dm^{-3} PhBu in *n*-BuCl purged with N_2.

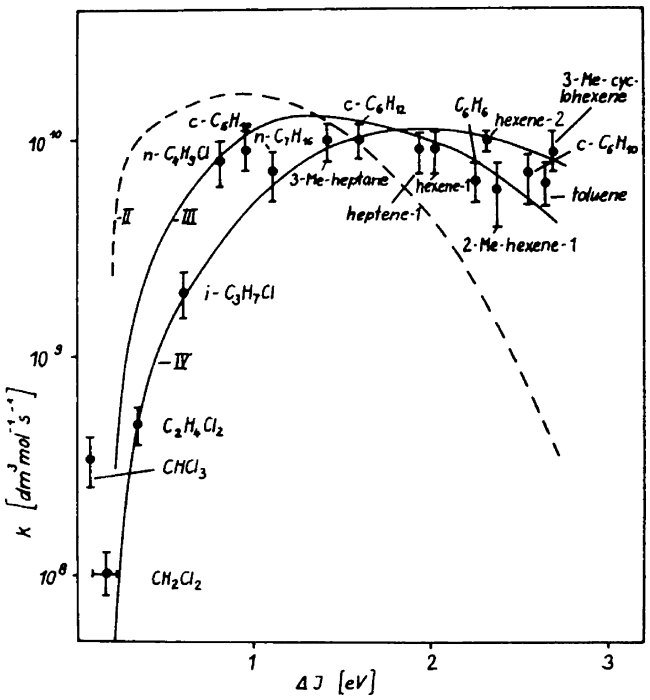

Figure 7. Dependence of the rate constant k_{ET} on ΔIP. Solid and dotted lines are calculated for different deformation energies as described in detail in ref 4. Reprinted with permission from ref 4. Copyright 1979 Bunsen Society.

with the use of an intermediary electron donor: the immediate formation of the phenoxyl radical (eq 2b) was quenched when benzene was added to the solution.[53] Again, the difference in IP_{gas} between phenol[54] and benzene is 0.7 eV.

In general, the observed behavior indicates a change in the mechanism of the electron-transfer gross reaction (1b): (i) At free energies ≥0.7 eV each collision (approach) of the reactants results in a prompt electron transfer. This is the FET case, where the two-product situation is the reflection of the molecule

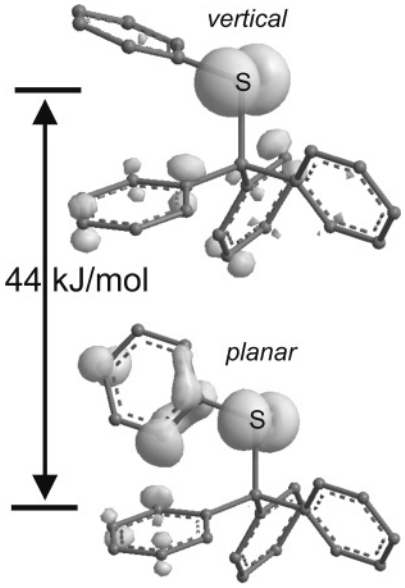

Figure 8. Spin density distribution of the radical cation (isospin 0.01) for **3** in the vertical and the planar conformation (H atoms are omitted).

SCHEME 5: Fragmentation after FET from the Different Conformers of Radical Cations

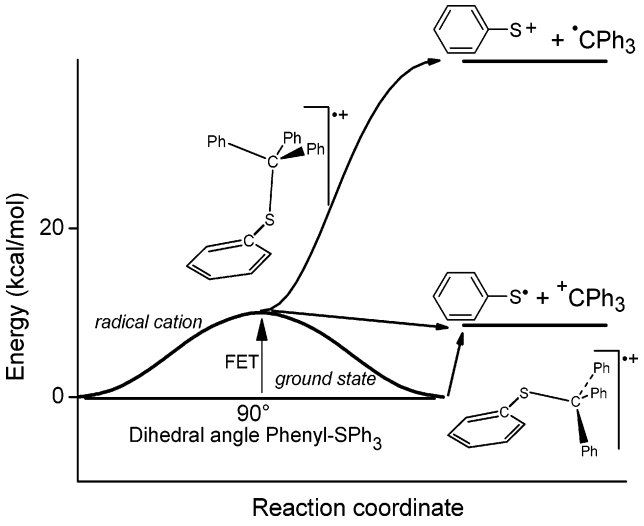

dynamics of the donor as reported in this paper. (ii) At $\Delta IP \leq 0.7$ eV, however, a normal reaction-controlled electron transfer happens (only with one product). Here, the collision number is >1, and therefore, within the approach of the reactants an energetically optimized encounter situation could be formed.

Interpretation by Means of Quantum Chemical Calculations. Aiming at a better understanding of the experimental results, we performed quantum chemical calculations on the neutral molecules and on their radical cations using the B3LYP/6-31G(d) method. Table 2 contains the data from the two radical cations that represent the extreme arrangements of the molecules. We chose to focus on them because they serve as good examples for the plethora of actual conformers of the solute sulfides.

The minimum energy geometries of the singlet ground state of compounds **1**−**3** have the S−C bond *perpendicular* to the phenyl ring plane. Nevertheless, the barrier for internal rotation is less than 3 kJ/mol, so in room temperature solutions there is practically an even distribution of the molecules between all possible angles. Free energy transfer takes place in a single step[4] and the radical cations are generated by having the same structure as the ground state molecules (vertical ionization). Contrary to the ground state, the equilibrium geometry of the radical cations is the one with the phenyl group positioned at the same plane with the aliphatic C atom (*planar* in Figure 8). This way a maximum overlap between the aromatic ring and the nonbonded S electrons is achieved. The activation barrier for rotation increases to 34−44 kJ/mol (see Table 2), and this energy difference can play the deciding role in the driving force for the subsequent fragmentation. Planar and vertical structures have a significantly dissimilar electron distribution of their highest molecular orbitals. The spin density in the structures of Figure 8 is shifted from the S atom (and the aromatic rings of the trityl group) (vertical form) to the Ar−S ring (planar form).

The process of FET is demonstrated in Scheme 5 for a ground state molecule with the minimum energy geometry: Ionization generates the radical cation with the least favorable conformation. An exothermic, one-step process (like the FET of eq 17) generates vibrationally excited states of the products.[4,55] This

$$n\text{-BuCl}^{\bullet+} + \text{PhSR} \rightarrow [n\text{-BuCl}]^{(*)} + [\text{PhSR}]^{\bullet+(*)}$$
$$^{(*)} = \text{vibrationally excited} \quad (17)$$

excessive energy results in a much smaller difference (than in Scheme 5) between $\mathbf{3}^{\bullet+}$ and the dissociation channel that yields the trityl radical.

Fragmentation of the unstable vertical radical cation of Scheme 5 takes place during the stretching motions of the transient that are much faster than its torsion oscillations (as can be seen in Table 2). There is a competition between dissociation and reorganization of the transient toward the metastable planar form. Once a transient adopts the planar form its mobility is drastically reduced because of the great rotation barrier. The unstable configuration of the radical cation cannot be repopulated backward. We conclude that reaction 15 arises exclusively from free energy transfer because it (FET) allows the formation of unstable and highly energetic transients.

5. Conclusions

Providing characteristic product distributions and variation of the free energy, the electron transfer from aromatic sulfides to the parent radical cations of *n*-butyl chloride enables a deeper insight into the mechanism of FET and allows us to distinguish between diffusion- and reaction-controlled process. We present here the first example of a FET reaction where there is a differentiation in the chemical behavior with the introduction of an additional reaction path. The low rotation barrier of aromatic sulfides provides the sample with an extended diversity of conformers. The vertical, unhindered free electron transfer reflects the dynamic profile of the ground state molecules directly to their radical cations. Some of the less stable conformers dissociate faster than they relax and this process is associated with the presence of two alternative fragmentation channels. Sulfides proved to be an ideal example of FET because the modification of the parent radical cation made it possible to obtain quantitative results about the yield of each of these channels. Furthermore, the variation of the free energy of the FET by stepwise electron transfer via different mediator molecules allows the energetic distinction between the diffusion-controlled (free) and the reaction-controlled transfer process. Whereas in the first one the rapid electron jump was characteristic for the product distribution, in the latter one the collision interaction of the reactants causes a delayed transfer via a reaction-controlled process.

Acknowledgment. We thank cordially Dr. Antonios Zarkadis (Ioannina, Greece) and Prof. Krzysztof Bobrowski (Warsaw) for many discussions and helpful proposals.

References and Notes

(1) Dorfman, L. M. *Acc. Chem. Res.* **1970**, *3*, 224.
(2) Mehnert, R. Properties in condensed Phases. In *Radical Ionic Systems*; Lund, A., Shiotani, M., Eds.; Kluwer Academic Publishers: Dordrecht, The Netherlands, 1991; p 231.
(3) Brede, O.; Mehnert, R.; Naumann, W. *Chem. Phys.* **1987**, *115*, 279.
(4) Mehnert, R.; Brede, O.; Bös, J.; Naumann, W. *Ber. Bunsen-Ges. Phys. Chem.* **1979**, *83*, 992.
(5) Brede, O.; Mahalaxmi, G. R.; Naumov, S.; Naumann, W.; Hermann, R. *J. Phys. Chem. A* **2001**, *105*, 3757.
(6) Mahalaxmi, G. R.; Hermann, R.; Naumov, S.; Brede, O. *Phys. Chem. Chem. Phys.* **2000**, *2*, 4947.
(7) Brede, O.; Hermann, R.; Naumann, W.; Naumov, S. *J. Phys. Chem. A* **2002**, *106*, 1398.
(8) Maroz, A.; Hermann, R.; Naumov, S.; Brede, O. *J. Phys. Chem. A* **2005**, *109*, 4690.
(9) Brede, O.; Maroz, A.; Hermann, R.; Naumov, S. *J. Phys. Chem. A* **2005**, *109*, 8081.
(10) Brede, O.; Hermann, R.; Naumov, S.; Zarkadis, A. K.; Perdikomatis, G. P.; Siskos, M. G. *Phys. Chem. Chem. Phys.* **2004**, *6*, 2267− 2275.
(11) Karakostas, N.; Naumov, S.; Siskos, M. G.; Zarkadis, A. K.; Hermann, R.; Brede, O. *J. Phys. Chem. A* **2005**, *109*, 11679.
(12) Brede, O.; Naumov, S. *J. Phys. Chem. A* **2006**, *110*, 11906.
(13) Schaefer, T.; Balejam, J. D. *Can. J. Chem.* **1986**, *64*, 1326.
(14) Baciocchi, E.; Gerini, F. *J. Phys. Chem. A* **2004**, *108*, 2332.
(15) Dewar, P. S.; Ernstbrunner, E.; Gilmore, J. R.; Godfrey, M.; Mellor, J. M. *Tetrahedron* **1974**, *30*, 2455.
(16) Potapov, V. K.; Kardash, I. E.; Sorokin, V. V.; Sokolov, S. A.; Evlasheva, T. I. *Khim. Vys. Energ.* **1972**, *6*, 392.
(17) Schweig, A.; Thon, N. *Chem. Phys. Lett.* **1976**, *38*, 482.
(18) Kimura, K.; Katsumata, S.; Achiba, Y.; Matsumoto, H.; Nagakura, S. *Bull. Chem. Soc. Jpn.* **1973**, *46*, 373.
(19) Yokoi, H.; Hatta, A.; Katsuya, I.; Sawaki, Y. *J. Am. Chem. Soc.* **1998**, *120*, 12728.
(20) Sumiyoshi, T.; Sakai, H.; Kawasaki, M.; Meiseki, K. *Chem. Lett.* **1992**, 617.
(21) Sumiyoshi, T.; Kawasaki, M.; Katayama, M. *Bull. Chem. Soc. Jpn.* **1993**, *66*, 2510.
(22) Chateauneuf, J. E. *Chem. Commun.* **1998**, 2099.
(23) Ioele, M.; Steenken, S.; Baciocchi, E. *J. Phys. Chem. A* **1997**, *101*, 2979.
(24) Baciocchi, E.; Del Giacco, T.; Gerini, M. F.; Lanzalunga, O. *Org. Lett.* **2006**, *8*, 641.
(25) Adam, W.; Argüello, J. E.; Peñéñory, A. B. *J. Org. Chem.* **1998**, *63*, 3905.
(26) Baciocchi, E.; Lanzalunga, O.; Malandrucco, S.; Ioele, M.; Steenken, S. *J. Am. Chem. Soc.* **1996**, *118*, 8973.
(27) Mehnert, R.; Brede, O.; Naumann, W. *Ber. Bunsen-Ges. Phys. Chem.* **1982**, *86*, 525.
(28) Becke, A. D. *J. Chem. Phys.* **1993**, *98*, 5648.
(29) Becke, A. D. *J. Chem. Phys.* **1996**, *104*, 1040.
(30) Lee, C.; Yang, W.; Parr, R. G. *Phys. Rev. B* **1988**, *37*, 785.
(31) Frisch, M. J.; Trucks, G. W.; Schlegel, H. B.; Scuseria, G. E.; Robb, M. A.; Cheeseman, J. R.; Zakrzewski, V. G.; Montgomery, J. A., Jr; Stratmann, R. E.; Burant, J. C.; Dapprich, S.; Millam, J. M.; Daniels, A. D.; Kudin, K. N.; Strain, M. C.; Farkas, O.; Tomasi, J.; Barone, V.; Cossi, M.; Cammi, R.; Mennucci, B.; Pomelli, C.; Adamo, C.; Clifford, S.; Ochterski, J.; Petersson, G. A.; Ayala, P. Y.; Cui, Q.; Morokuma, K.; Salvador, P.; Dannenberg, J. J.; Malick, D. K.; Rabuck, A. D.; Raghavachari, K.; Foresman, J. B.; Cioslowski, J.; Ortiz, J. V.; Baboul, A. G.; Stefanov, B. B.; Liu, G.; Liashenko, A.; Piskorz, P.; Komaromi, I.; Gomperts, R.; Martin, R. L.; Fox, D. J.; Keith, T.; Al-Laham, M. A.; Peng, C. Y.; Nanayakkara, A.; Challacombe, M.; Gill, P. M. W.; Johnson, B.; Chen, W.; Wong, M. W.; Andres, J.; Gonzalez, C.; Head-Gordon, M.; Replogle, E. S.; Pople, J. A. *Gaussian 03*, revision B.02 Gaussian: Pittsburgh, PA, 2003.
(32) Engman, L.; Lind, J.; Merenyi, G. *J. Phys. Chem.* **1994**, *98*, 3174.
(33) Bartl, L.; Steenken, S.; Mayr, H.; McClelland, R. A. *J. Am. Chem. Soc.* **1990**, *112*, 6918.
(34) Wang, Y.; Trla, J. J.; Dorfman, L. M. *J. Phys. Chem.* **1979**, *83*, 1946.
(35) Bromberg, A.; Schmidt, K. H.; Meisel, D. *J. Am. Chem. Soc.* **1984**, *106*, 3056.
(36) Hadel, L. M.; Platz, M. S.; Scaiano, J. C. *J. Am. Chem. Soc.* **1984**, *106*, 283.
(37) Faria, J. L.; Steenken, S. *J. Am. Chem. Soc.* **1990**, *112*, 1277.
(38) Bromberg, A.; Schmidt, K. H.; Meisel, D. *J. Am. Chem. Soc.* **1985**, *107*, 83.
(39) Gleiter, R.; Heilbronner, E.; Hornung, V. *Angew. Chem., Int. Ed. Engl*. **1970**, *9*, 901.
(40) Brede, O.; Bös, J.; Helmstreit, W.; Mehnert, R. *Radiat. Phys. Chem.* **1982**, *19*, 1.
(41) Brede, O.; Mehnert, R.; Naumann, W.; Cserep, G. y. *Radiat. Phys. Chem.* **1982**, *20*, 155.
(42) Akiyama, I.; Li, K. C.; LeBreton, P. R.; Fu, P. P.; Harvey, R. G. *J. Phys. Chem.* **1979**, *83*, 2997.
(43) Brede, O.; Bös, J.; Naumann, W.; Mehnert, R. *Radiochem. Radioanal. Lett.* **1978**, *35*, 85.
(44) Baciocchi, E.; Del Giacco, T.; Giombolini, P.; Lanzalunga, O. *Tetrahedron*, in press.
(45) Claridge, R. F. C.; Fischer, H. *J. Phys. Chem.* **1983**, *87*, 1960.
(46) Fujisaki, N.; Comte, P.; Gäumann, T. *J. Chem. Soc., Chem. Commun.* **1993**, 848.
(47) Popielarz, R.; Arnold, D. R. *J. Am. Chem. Soc.* **1990**, *112*, 3068.
(48) Connors, K. A. *Chemical Kinetics: The study of reaction rates in solution*; VCH Publishers: New York, 1990; p 62.
(49) Palmer, T. F.; Lossing, F. P. *J. Am. Chem. Soc.* **1962**, *84*, 4661.
(50) Harrison, A. G.; Lossing, F. P. *J. Am. Chem. Soc.* **1960**, *82*, 1052.
(51) Doa, Q. T.; Elothmania, D.; Guillanton, G. L.; Simonet, J. *Tetrahedron Lett.* **1997**, *38*, 3383.
(52) Nagy-Felsobuki, E.; Peel, J. B. *J. Electron Spectrosc. Relat. Phenom.* **1979**, *16*, 379.
(53) Brede, O.; Naumov, S.; Hermann, R. *Radiat. Phys. Chem.* **2003**, *67*, 225.
(54) Lipert, R. J.; Colson, S. D. *J. Chem. Phys.* **1990**, *92*, 3240.
(55) Medvedev, E. S.; Osherov, V. I. *Radiationless Transitions in Polyatomic Molecules*; Springer Series in Chemical Physics 57; Springer: Berlin, 1995; p 36.